JOURNAL OF SOLID STATE CHEMISTRY 1, 229–236 (1970)

X-Ray Spectroscopic Studies of Bonding in Transition Metal Germanides †

A. E. AUSTIN AND E. ADELSON

Battelle Memorial Institute, Columbus Laboratories, 505 King Avenue, Columbus, Ohio 43201

Received September 3, 1969

The electronic structure of transition metal germanides has been studied by X-ray spectroscopy. The germanides were the $M_{1.67}Ge$, MGe and MGe_2 compounds, where M was Ni, Co, Fe, Mn. The changes in distribution of the $3d$–$4s$–$4p$ bonding electrons for both the metal and germanium were investigated by measurement of the $K\beta_5$ X-ray spectrum intensity and shape. The intensities of the $K\beta_5$ spectra of Fe, Co, and Ni increased in the germanides. This indicates increased overlap of the metal $3d$–$4p$ electrons. The intensities of the germanium $K\beta_5$ and the manganese $K\beta_5$ spectra decreased in the germanides. The $K\beta_5$ intensities have been correlated with regard to specific molecular orbitals involving the symmetry of the covalent metal–germanium bonds in the compounds.

Introduction

Studies of the $K\beta_5$ X-ray emission spectra of iron germanides (*1*) have shown that the intensities of the spectra can be correlated with possible molecular orbitals and with the magnetic properties of these compounds. Similar studies of transition metals (*2*) have shown that the total $K\beta_5$ intensities when plotted versus atomic number yield a graph which is the inverse of the Slater-Pauling curve (*3*). Since the transition metal germanides exhibit varying magnetic properties ranging from Pauli paramagnetism through ferrimagnetic and antiferromagnetic structures, it was of interest to see how the spectra of these compounds were related to bonding and magnetic properties.

The $K\beta_5$ spectra are due to transitions from the $3d$–$4s$–$4p$ band to the $1s$ level. In particular, Nemoshkalenko and Nagornyi (*4*) have verified that it is the admixture of p states in the conduction band which gives rise to the $K\beta_5$ spectra, as opposed to quadrupole transitions. Therefore, when covalent bonding causes an increased p admixture in a $3d$ metal band, the $K\beta_5$ spectra will increase in intensity. Since the $3p$ electrons of the metal remain localized, the $K\beta_{1,3}$ spectra, which are due to $3p$–$1s$ transitions, can be used for normalization. For germanium the $K\beta_2$ spectra of the $4p$ to $1s$ transition also serve as a measure of possible variations in germanium $4p$ electrons.

Germanium and the transition metals Mn, Fe, Co, and Ni form compounds $M_{1.67}Ge$ (M = Mn, Fe, Co, Ni), MGe (M = Fe, Co, Ni), and MGe_2 (M = Fe, Co). The $M_{1.67}Ge$ compounds are isostructural and of the hexagonal $B8_2$ and $D8_8$ types which have two metal sublattices. These have nearest neighbor coordination of 14 for one type of metal atom and 11 for the other metal atom and Ge. The MGe compounds have structures basically related to the hexagonal NiAs type with tenfold coordination about metal atoms and sixfold coordination for Ge. The MGe_2 compounds, although not isostructural, are similar in having eight Ge nearest neighbors about each metal atom, each of which has two nearest neighbor Fe atoms in $FeGe_2$ but one nearest neighbor Co atom in $CoGe_2$. This sequence of metal germanides permits one to study the dependence of the $3d$–$4p$ electron overlap both on an increasing number of germanium nearest neighbors and on the number of $3d$ electrons.

A number of ternary compounds of $B8_2$ type also exist in these systems. Of these, the compounds $Mn_{.9}Fe_{.9}Ge$, $Fe_{1.67}Co_{1.67}Ge$ and CoMnGe are ordered, and therefore the spectra from the two different metal sites in the $M_{1.67}Ge$ type can be separated. The crystal structures and magnetic

† This research was sponsored by the Air Force Office of Scientific Research, Office of Aerospace Research, United States Air Force, under Grant Number AF-AFOSR-262-66.

TABLE I

PROPERTIES OF THE TRANSITION METAL GERMANIDES

Compound	Space Group	Type[a]	Magnetism[b]	$\bar{\mu}$/Metal	Reference
Ni	Fm3m	$A1$	F	0.6	*5*
$Ni_{1.67}Ge$	$P6_3/mmc$	$B8_2$	PP	—	*6*
NiGe	Pnma	$B31$	P	—	*7*
Co	Fm3m	$A1$	F	1.75	*5*
$Co_{1.67}Ge$	$P6_3/mmc$	$B8_2$	PP	—	*6*
CoGe	C^2/m	—	P	—	*8*
$CoGe_2$	Aba^2	Ce	P	—	*9*
CoMnGe	$P6_3/mmc$	$B8_2$	F	1.8	—
$Fe_{1.67}Co_{1.67}Ge$	$P6_3/mmc$	$B8_2$	F	0.85	*10*
Fe	Im3m	A_2	F	2.2	*5*
$Fe_{1.60}Ge$	$P6_3/mmc$	$B8_2$	F	1.5	*11*
FeGe	P6/mmm	$B35$	AF	1.7	*11, 12*
$FeGe_2$	I^4/mcm	$C16$	AF	0.7	*11, 13*
$Fe_{.9}Mn_{.9}Ge$	$P6_3/mmc$	$B8_2$	F	0.8	*14, 15*
Mn	$I\bar{4}3m$	$A12$	AF	1.1	*5, 16*
Mn_5Ge_3	$P6_3/mcm$	$D8_8$	F	2.4	*17, 18, 19*
Mn_3Ge_2	—	—	AF	2.3	*19*

[a] Strukturbericht Type.
[b] F—ferro- or ferrimagnetic, P—paramagnetic, PP—Pauli paramagnetic, AF—anti-ferromagnetic.

properties of these compounds are listed in Table I. The magnetic moment of a transition metal decreases with an increase in coordination, a decrease of metal–metal bonds and an increase of metal–germanium bonds. This is apparent in the sequence of iron germanides. These changes in coordination and bonding also can lead to the transition from ferrimagnetism to antiferromagnetism.

In our earlier studies (*1*, *2*), we found that the magnetic moments of the iron germanides and transition metals were related to the $K\beta_5$ intensities. Therefore, it is of interest also to determine the relationship between the moments of the other transition metal germanides and their $K\beta_5$ spectra.

Further, because covalent bonding is expected to be of great importance in determining the properties of these compounds, we have obtained possible molecular orbitals of the bonding electrons from the irreducible representations of the point groups. It should be noted that the molecular orbitals, a representation on an angular momentum basis, are equivalent to a representation employing the coordination distances between atomic sites and that therefore the crystallographic symmetry properties are directly related to the physical properties through the MOs.

Experiment and Results

The spectrometer used to obtain the data has been described heretofore (*1*). It consists of a high-resolution single-crystal rocking spectrometer, with a stepping increment of 0.0025 degree, mounted on a Jarrell-Ash microfocus unit. The resolution, $\lambda/\delta\lambda$, is 6,460 for the iron $K\beta_5$ spectra. The method of target preparation is also described in Ref. (*1*). The compounds used were prepared similarly to the iron germanides (*11*) and were all single phase according to their X-ray diffraction patterns.

The $K\beta_5$ and $K\beta_{1,3}$ spectra were obtained for the metal atoms in all the compounds which are listed in Table I, and the $K\beta_{2,5}$ and $K\beta_{1,3}$ spectra for germanium in the same compounds. For each compound, the $K\beta_5$ spectrum was normalized to the $K\beta_{1,3}$ spectrum, and was then corrected for the

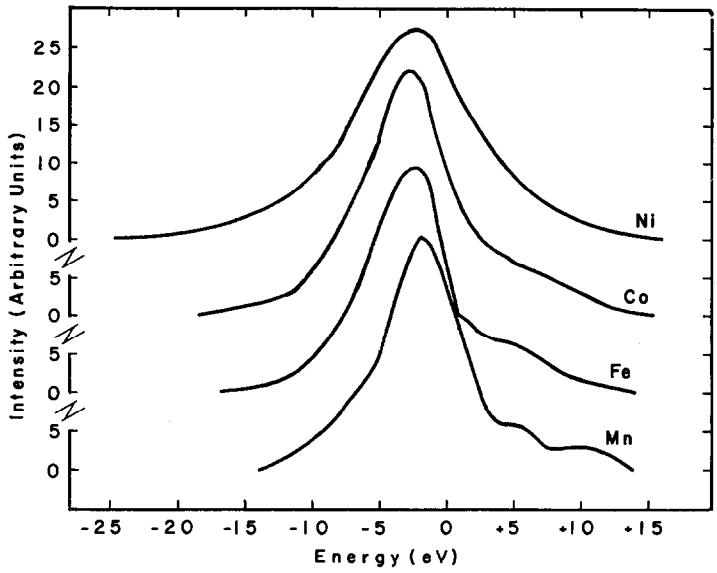

FIG. 1. $K\beta_5$ spectra of Ni, Co, Fe, and Mn.

background of the latter. Then the transition metal spectra were planimetered after subtraction of background, and for iron and cobalt the area under the $K\beta'''$ satellite (*21*), which is presumably due to the presence of oxygen, was not included. Similarly, we did not attempt to interpret the high energy structure of the Mn $K\beta_5$ spectrum of the metal since it was not entirely certain that the structure was real.

The statistical counting error, $1/\sqrt{n}$, where n is the counts, is 0.0316 for 1000 counts, the minimum number obtained at any point. Energy increments were of the order of 1 eV. Therefore, the statistical error in each total $K\beta_5$ intensity is less than 1%. However, the error in extrapolating the background is estimated to be 3%, for relative measurements, since the same method was used in every case. Possible systematic errors in the background have not been evaluated. In addition, a possible 3% error is introduced by planimetering, and an error of 1% in normalizing to the $K\beta_{1,3}$ peak. Therefore, we take ±5% as the combined error with respect to the precision of the intensity measurements. The absolute accuracy of the set of data may, however, not be as good.

In estimating the error in widths, the probable error in the spectrometer advance mechanism was combined with the statistical counting error. The resultant errors, roughly 6–7%, reflect the average 5% error in our ability to locate any one point in the stepping drive.

The $K\beta_5$ spectra with background subtracted for the metals, the $M_{1.67}Ge$ and the MGe compounds are shown in Figs. 1, 2, and 3, respectively. The zeros of the energy scale are the Fermi levels in the respective metals. These have been obtained by comparing the energies of $K\beta_{1,3}$ spectra with the absorption data listed in Bearden's (*20*) table. The results are summarized in Table II, in which the areas of the $K\beta_5$ spectra, $\int I(E)dE$, the distances from the $K\beta_{1,3}$ spectra, the half-widths and the ratios of intensities are given. In Fig. 1, the $K\beta_5$ spectra of the metals Ni and Co are fairly symmetrical while those of Fe and Mn show a steep edge on the high energy side. The Ni spectrum shows a marked increase in width compared to the other metals. In Fig. 2, which shows the spectra of the $M_{1.67}Ge$ compounds, the $CoK\beta_5$ spectrum is broader by about 2 eV than in the metal. In addition, increased intensity of the spectra is demonstrated. Here the peak position of the Ni $K\beta_5$ is increased by 1.4 eV. In Fig. 3, which presents the spectra of the MGe compounds, a further increase in intensity for Fe, Ni, and Co and increased breadth for the latter two spectra is shown as compared to the spectra of the $M_{1.67}Ge$ compounds and of the metals.

The integrated intensities of the metal $K\beta_5$ spectra increased up to 30% in going from the metal to the germanides in the order $M_{1.67}Ge$, MGe, and MGe_2, except for manganese where there was a decrease. Our interpretation is that the increased intensity is due to increased p electron overlap of the $3d$ electrons.

For germanium, the stronger $K\beta_2$ overlaps the

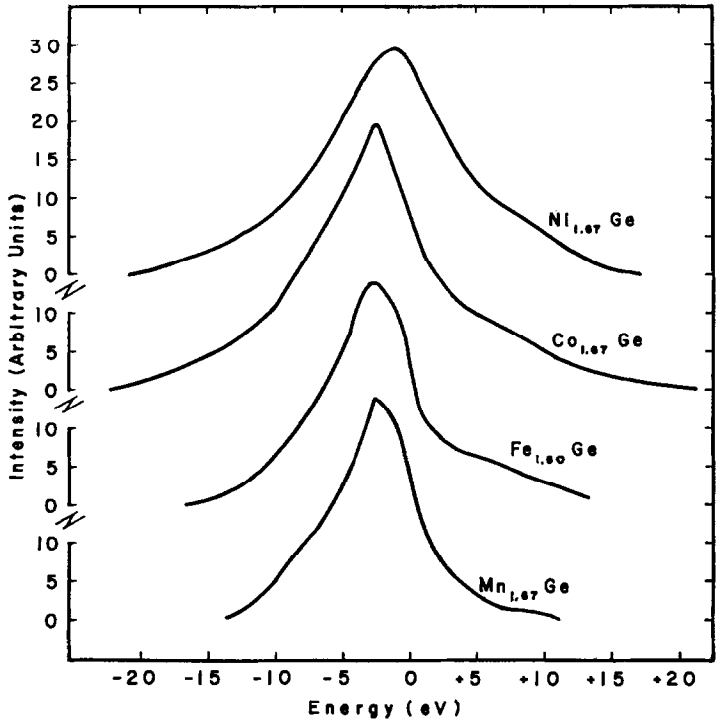

FIG. 2. $K\beta_5$ spectra of Ni, Co, Fe, and Mn in their $M_{1.67}Ge$ compounds.

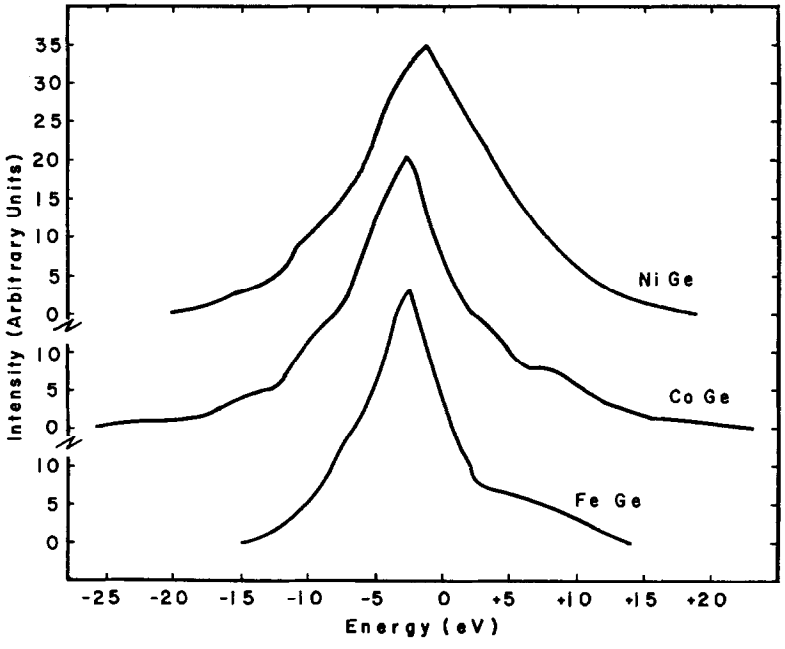

FIG. 3. $K\beta_5$ spectra of Ni, Co, Fe, in their MGe compounds.

$K\beta_5$ line so that it is necessary to reflect the $K\beta_2$ symmetrically in order to obtain the background under the $K\beta_5$. A small spurious peak which often appears on the side of the $K\beta_5$ from this procedure has been ignored in obtaining the germanium $K\beta_5$ intensities. Since the resultant $K\beta_5$ is a wide band without a clear peak, the distance from the $K\beta_{1,3}$ to the $K\beta_2$ has been measured in each case. The

TABLE II

$K\beta_5$ DATA FOR NICKEL, COBALT, AND IRON

Compound	$I(K\beta_5)$	Half Width, eV	Separation $K\beta_5K\beta_{1,3}$, eV	$\frac{I\text{ cpd}}{I\text{ metal}}$
Ni	4.49	13.1 ± .8	63.1	1.00
$Ni_{1.67}Ge$	5.13	13.3 ± .8	64.5	1.14
NiGe	6.10	14.2 ± .9	64.3	1.36
Co	3.67	9.2 ± .7	56.5	1.00
$Co_{1.67}Ge$	5.01	11.1 ± .8	56.6	1.36
CoGe	4.97	10.5 ± .8	56.3	1.35
$CoGe_2$	5.43	13.0 ± 1.0	56.8	1.48
CoMnGe	4.18	12.7 ± .9	55.6	1.14
$Fe_{1.67}Co_{1.67}Ge$	4.91	12.7 ± .9	56.0	1.34
Fe	2.96	8.2 ± .6	49.7	1.00
$Fe_{.9}Mn_{.9}Ge$	3.38	8.9 ± .6	49.9	1.14
$Fe_{1.60}Ge$	3.19	8.8 ± .6	49.7	1.08
FeGe	3.50	8.2 ± .6	50.0	1.18
$FeGe_2$	3.84	9.3 ± .7	49.8	1.30
$Fe_{1.67}Co_{1.67}Ge$	2.94	8.1 ± .6	50.7	0.994
Mn	3.45	9.9 ± .6	44.2	1.00
Mn_5Ge_3	3.09	9.7 ± .6	43.6	0.894
Mn_3Ge_2	2.90	8.1 ± .6	43.7	0.840
$Fe_{.9}Mn_{.9}Ge$	2.92	8.8 ± .6	43.7	0.845
CoMnGe	3.17	7.1 ± .5	43.7	0.917

TABLE III

GERMANIUM $K\beta_5$ DATA

Compound	$I(K\beta_5)$	Half Width, eV	Separation $K\beta_2$–$K\beta_{1,3}$, [a] eV	$\frac{I\text{ cpd}}{I\text{ Ge}}$	$I(K\beta_2)$
Ge	1.44	31.5	118.1	1.00	3.44
$FeGe_2$	1.14	26.0	116.7	0.79	3.73
$CoGe_2$	1.10	21.7	118.5	0.765	3.76
FeGe	1.09	25.9	120.3	0.76	3.03
CoGe	1.13	27.2	118.9	0.785	3.67
NiGe	1.06	22.4	117.1	0.735	4.54
$Mn_{1.5}Ge$	1.13	24.9	119.1	0.785	3.64
$Mn_{1.67}Ge$	1.08	24.9	116.3	0.75	3.77
$Fe_{1.60}Ge$	0.90	21.7	118.8	0.625	3.08
$Co_{1.67}Ge$	1.05	26.7	120.0	0.73	4.09
$Ni_{1.67}Ge$	0.92	24.0	119.3	0.64	3.71
$Fe_{1.67}Co_{1.67}Ge$	1.05	29.2	118.7	0.73	3.62
$Fe_{.9}Mn_{.9}Ge$	0.87	27.5	117.3	0.60	2.93
CoMnGe	0.78	20.8	120.9	0.54	3.57

[a] ±.7 eV for all data in this column.

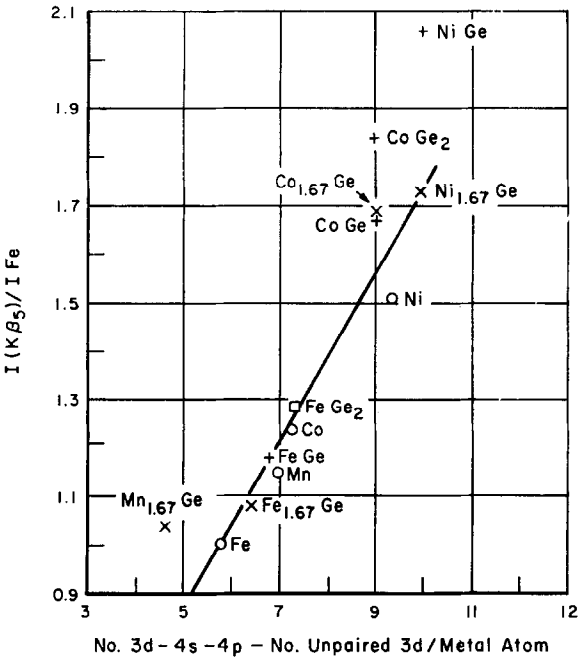

FIG. 4. Plot of relative $IK\beta_5$ versus the number of $3d + 4s + 4p$ valence electrons per metal atom.

intensities and half-widths for germanium are listed in Table III.

The data in Table III show that the ratios of the germanium $K\beta_5$ intensities in the compounds to that of pure germanium decrease as the transition metal content increases. Therefore, there either is electron transfer of germanium $4p$ electrons to the metal or an increased separation of the $3d$ and $4p$ bands at the germanium sites in the compounds. In the former case, the $K\beta_2$ intensity of the $4p$–$1s$ transition ought to decrease as the metal content increases. The data in Table III indicate that this does not occur, in spite of the large spread in values due to the uncertainties introduced in obtaining background, subtracting the $K\beta_5$ and planimetering.

Therefore, the transition metal $K\beta_5$ intensities measure the distribution of electrons in the $3d$–$4s$–$4p$ band through the $3d$–$4p$ overlap. Most of these compounds are magnetic, and it is generally assumed that the $3d$ electrons producing the moment are localized. If this is correct, the intensities will be proportional to the number of electrons in the conduction-valence band. This is shown in Fig. 4, where the ratios of the intensities to that of iron are plotted against the number of nonmagnetic d electrons plus the $4s$ and $4p$ contribution (which is assumed to be constant for these metals). It is seen that such a correlation succeeds in relating most of the data.

Discussion

In the previous section, it was shown that the intensities of the $K\beta_5$ spectra are highly correlated with the nonlocalized d electrons. On the other hand, the $K\beta_5$ spectra arise from overlapping $3d$ and $4p$ bands. The distribution of d and p electrons is determined by the bonding, which is a qualitative way of describing the proper basis for the electronic valence states (*22*). The crystallographer's implicit assumption is that a r basis, e.g. (xyz), is physically meaningful, but this is completely equivalent to an (r, θ, ϕ) basis. The latter is more meaningful for the description of dipole transitions between at least partially localized states. However, the group properties of the former are more easily derived. Nonetheless, the symmetry properties of the one are completely equivalent to those of the other. We can use the spatial symmetries to obtain the irreducible representations of the point groups which are realized physically. Then, we can correlate the covalent bonding, which is determined by (partially) localized electrons, with the irreducible representations of the point groups since these give the possible distributions of angular momentum states.

Assuming that each possible state is equally occupied, we had noted previously (*1*) that the intensities were proportional to the sum of possible $d+p$ states. For those compounds, the iron germanides, we had taken an average over the possible symmetry states. However, to obtain agreement with the nickel and cobalt data, particular symmetry combinations must be chosen to fit the bed of Procrustes provided by the assumption of equal occupancy. These are listed in Table IV, for the metal in the iron, metal, and cobalt compounds along with the $d+p$ fractions, their ratios to those of the pure metals, and the ratios of the intensities in the compounds to the intensities of the pure metals. Because of the structural complexity of manganese, the appropriate irreducible representations have not yet been calculated. In the $M_{1.67}Ge$ compounds, the incomplete occupancy of the metal d site has been considered in calculating the $d+p$ fraction, but the maximum coordination has been used for the bond and orbital. Since each metal 1–metal 2 orbital had to agree with the metal 2–metal 1 bond and both metals had to meet a similar requirement for bonds with germanium, the number of choices is not as great as it otherwise might be.

Excellent agreement is obtained in this way between the calculated and experimental ratios. This agrees with the correlation shown in the last section in which the ratios were roughly proportional to

TABLE IV

SYMMETRY COMBINATIONS

Compound	Bond	Orbital (s)	Fraction $d+p$	Ratio to metal	$\frac{I\,\text{cpd}}{I\,\text{metal}}$
Fe	Fe–8Fe	d^3fsp^3	0.750	1.00	1.00
$Fe_{.9}Mn_{.9}Ge$	Fe–5Ge	d^4p	0.874	1.165	1.14
	Fe–6Mn*	d^2sp^3			
	Fe–4Fe*	p^2ds			
$Fe_{1.60}Ge$	Fe_I–2Fe_I	sp	0.819	1.09	1.08
	Fe_I–6Fe_{II}*	d^2p^3s			
	Fe_I–6Fe_{II}*	d^2p^3s			
	Fe_{II}–5Ge*	d^4p			
	Fe_{II}–6Fe_I*	d^2sp^3			
	Fe_{II}–4Fe_{II}*	p^2ds			
FeGe	Fe–6Ge	d^2sp^3	0.900	1.20	1.18
	Fe–4Fe	d^2p^2			
$FeGe_2$	Fe–8Ge	d^5p^3 or d^4sp^3	0.945	1.27	1.27
	Fe–2Fe	d^2p^2			1.32
$(FeCo)_{1.67}Ge$	Fe–2Fe	sp	0.75	1.00	0.994
	Fe–6Ge	d^2sp^3			
	Fe–6Co*	d^2p^2			
Co	Co–12Co	$sp^3d^5f^3$	0.667	1.00	1.00
$Co_{1.67}Ge$	Co_I–2Co_I	dp	0.894	1.34	1.36
	Co_I–6Ge	d^2sp^3			
	Co_I–6Co_{II}*	d^3p^3			
	Co_{II}–5Ge*	d^3sp			
	Co_{II}–6Co_I*	d^3p^3			
	Co_{II}–4Co_{II}*	p^2ds			
CoGe	Co–4Co	d^2p^2	0.900	1.35	1.35
	Co–6Ge	d^2sp^3			
$CoGe_2$	Co_I–Co_{II}	d or p	1.000	1.47	1.48
	Co_I–4Ge_I	p^2d^2 or pd^3			
	Co_I–4Ge_{II}	pd^3 or p^2d^2			
	Co_{II}–4Ge_I	p^2d^2 or pd^3			
	Co_{II}–4Ge_{II}	pd^3 or p^2d^2			
CoMnGe	Co–6Mn	d^2sp^3	0.800	1.20	1.14
	Co–5Ge	d^3sp			
	Co–4Co	p^2ds			
$(FeCo)_{1.67}Ge$	Co–6Fe*	d^3p^3	0.921	1.38	1.36
	Co–5Ge*	d^3ps			
	Co–4Co*	d^2p^2			
Ni	Ni–12Ni	$sp^3d^5f^3$	0.667	1.00	1.00

TABLE IV—*continued*

Compound	Bond	Orbital (s)	Fraction $d+p$	Ratio to metal	$\frac{I\text{ cpd}}{I\text{ metal}}$
$Ni_{1.67}Ge$	Ni_I–$2Ni_I$	dp			
	Ni_I–6Ge	d^2sp^3	0.837	1.115	1.14
	Ni_I–$6Ni_{II}$*	d^2sp^3			
	Ni_{II}–$6Ni_I$	d^2sp^3			
	Ni_{II}–5Ge	d^3sp			
	Ni_{II}–$4Ni_{II}$*	p^2ds			
NiGe	Ni–Ge	d^2sp^3	0.900	1.35	1.36
	Ni–4Ni	d^2p^2			

* Does not include corrections to total number of bonds due to occupancy.

nonmagnetic $d+p$ electrons. If there were not so many possibilities, it would be possible to assign occupancies to the orbitals given here. However, properly symmetrized functions would first have to be constructed.

Conclusion

The X-ray $K\beta_5$ spectra of the transition metals depend on the $3d$–$4p$ electron overlap in their compounds. The metal $K\beta_5$ intensities in the germanides of Ni, Co, and Fe increase up to 30% with increasing germanium content, as in MGe_2, while the opposite effect occurs in the germanium $K\beta_5$ spectra. The manganese germanides exhibit the opposite effect. The $K\beta_5$ intensities of the transition metals and their compounds increase with the number of $3d+4s+4p$ valence electrons per metal atom for iron, manganese, cobalt, and nickel.

Although it is difficult to distinguish between metallic bonding and covalency quantitatively, some qualitative distinctions can be drawn. Because the germanium $K\beta_2$ spectra indicate that there is no electron transfer to the metals which can be correlated with intensities, the changes in metal $K\beta_5$ spectra must be due principally to redistribution of electrons at the metal site. This is obvious in the magnetic moments which are a direct result of this redistribution and which were employed to obtain the correlation between intensity ratios and nonmagnetic electrons. This change in occupancy of the bands is more likely due to shifting of the bands rather than a redistribution of electrons in rigid bands.

References

1. E. ADELSON AND A. E. AUSTIN, X-Ray Spectroscopic Studies of Bonding in Iron Germanides, *Advan. X-Ray Analysis* **12**, 506 (1969).
2. E. ADELSON AND A. E. AUSTIN, to be published.
3. L. PAULING, "The Nature of the Chemical Bond," 3rd ed., p. 398, Cornell University Press, New York, 1960.
4. V. V. NEMOSHKALENKO AND V. YA. NAGORNYI, *Sov. Phys. Dokl.* **12**, 735 (1968).
5. W. B. PEARSON, "A Handbook of Lattice Spacings and Structures of Metals and Alloys", Vol. 1, Pergamon Press, Inc., New York, 1958.
6. K. KANEMATSU, K. YASUKOCHI, AND T. OHOYAMA, *JPSJ* **17**, 932 (1962).
7. H. PFISTERES AND K. SCHUBERT, *Z. Metallk.* **41**, 358 (1950).
8. S. BHAN AND K. SCHUBERT, *Z. Metallk.* **51**, 327 (1960).
9. H. PFISTERES AND K. SCHUBERT, *Z. Metallk.* **41**, 433 (1950).
10. K. KANEMATSU, K. YASUKŌCHI, AND T. OHOYAMA, *JPSJ* **17**, 1932 (1962).
11. E. ADELSON AND A. E. AUSTIN, *J. Phys. Chem. Sol.* **26**, 1795 (1965).
12. H. WATANABE AND N. KUNITOMI, *JPSJ* **21**, 1932 (1966).
13. J. B. FORSYTH AND C. E. JOHNSON, *Phil. Mag.* **10**, 713 (1964).
14. T. SUZUOKA, E. ADELSON, AND A. E. AUSTIN, *Acta Cryst.* **A24**, 513 (1968).
15. A. E. AUSTIN, *J. Appl. Phys.* **40**, 1381 (1969).
16. J. S. KASPER AND B. W. ROBERTS, *Phys. Rev.* **101**, 537 (1956).
17. R. CISZEWSKI, *Phys. Stat. Sol.* **3**, 1999 (1963).
18. L. CASTELLIZ, *Mh. Chem.* **84**, 765 (1953).
19. R. FONTAINE ET R. PAUTHENET, *Compt. Rend.*, **254**, 650 (1962).
20. J. A. BEARDEN, "X-Ray Wavelengths," U.S. Atomic Energy Commission Report NYO-10586.
21. K. M. KOLOBOVA, A. Z. MEN'SHIKOV, AND S. A. NEMNONOV, *Fiz. Metal. Metalloved* **21**, 618 (1966).
22. S. KURTIN, T. C. MCGILL, AND C. A. MEAD, *Phys. Rev. Letters* **22**, 1433 (1969).